

Theory of neutral nitrogen-vacancy center in diamond and its qubit application

Adam Gali¹

¹*Department of Atomic Physics, Budapest University of Technology and Economics, Budafoki út 8., H-1111, Budapest, Hungary*

The negatively charged nitrogen-vacancy defect (NV)⁻ in diamond has attracted much attention in recent years in qubit and biological applications. The negative charge is donated from nearby nitrogen donors that could limit or stem the successful application of (NV)⁻. In this Letter, we unambiguously identify the *neutral* nitrogen-vacancy defect (NV⁰) by *ab initio* supercell calculations. Our analysis shows that i) the spin state can be *selectively* occupied optically, ii) the electron spin state can be manipulated by time-varying magnetic field, and iii) the spin state may be read out optically. Based on this NV⁰ is a new hope for realizing qubit in diamond *without* the need of nitrogen donors.

Realization of qubits is of extremely high importance because that can be used in quantum cryptography, quantum optics and quantum computing. One of the most promising candidate is the *negatively charged* nitrogen-vacancy defect (NV⁻) [1, 2] that can operate at *room temperature* [3, 4, 5, 6, 7, 8, 9, 10, 11]. The negative charge is donated from nitrogen substitutional (N_S) [12, 13]. It has been very recently shown that the major source of the decoherence of the electron spin of the negatively charged NV center is the electron spin bath of nitrogen substitutionals in type-*Ib* diamond, that can be eliminated only at low temperature using a giant magnetic field [14]. This is a serious limiting factor towards the development for *practical* applications. In addition, it has been recently demonstrated that nanometer-sized diamond particles containing NV⁻ are useful as fluorescent biomarkers for *in vitro* imaging applications [15, 16]. However, the requirement of the extra charge on NV defect from N_S could be critical in biomarker applications, where the size of the nanodiamond is reduced to some nanometers in diameter [17]. One solution of this problem would be to apply the paramagnetic *neutral* NV defect (NV⁰) which produces strong photoluminescence at 2.156 eV (similar to NV⁻) and it *does not require an extra electron*. The NV⁻ center is well identified [12] while its strong connection to its neutral counterpart is well established experimentally [18, 19, 20]. However, the overall knowledge about NV⁰ is scarce. Very recently, an $S = \frac{3}{2}$ electron paramagnetic resonance (EPR) center has been found in photo-excited diamond doped by ¹⁵N [21]. A sizeable ¹⁵N hyperfine constants have been detected in the EPR measurements and it was proposed that the signal was originated from one of the excited states of NV⁰ [21]. We emphasize that the identification of the EPR signal of NV⁰ is a *key step* in order to apply it for qubit, and to trace it magnetically in biomarker applications.

In this Letter we i) unambiguously *identify* the EPR signal of NV⁰ ii) provide a detailed spin density distribution around the defect; the results indicate that the defect states are well-localized and the electron spin can be decoupled from the spin bath of ¹³C nuclei iii) analyze the electronic structure by group theory explaining the photo-excitation of NV⁰; this shows that the $M_S = \pm 1/2$ sublevels are *selectively* occupied in the photo-ionization process and appropriate microwave magnetic field can be applied to choose also selectively ei-

ther $M_S = +3/2$ or $M_S = -3/2$ which finally can be used as qubit iv) we propose that the $M_S = +3/2$ or $M_S = -3/2$ states may be read out optically during the emission process from the excited state to the ground state. This gives a hope for realization of qubit by NV⁰ defect.

We employed density functional theory calculations with local density approximation (LDA) using a large, 512-atom simple cubic diamond supercell. We used two different codes: the geometry of the defect was optimized with the VASP code [22] while the hyperfine tensors of NV⁰ were calculated by the CPPAW code [23]. Both VASP and CPPAW codes apply the all-electron PAW method and plane wave basis set. We used a cut-off of 30 Ry and Γ -point for k-point sampling. Other details and references can be found in our previous publication [24] where we could successfully describe the negatively charged NV center and can reproduce well the experimental hyperfine data.

The NV defect has C_{3v} symmetry, if no reconstruction occurs. We use defect-molecule and group theory analysis below as for NV⁻ (c.f. [24] and references therein). Four dangling bonds point to the vacant site resulting in $a_1(1)^2 a_1(2)^2 e^1$ configuration for the neutral defect, where $a_1(2)^2$ and the double degenerate e^1 appear in the fundamental band gap. In this configuration, the system is basically Jahn-Teller unstable because the degenerate state is only partially filled by electrons. The static Jahn-Teller effect would result in C_{1h} symmetry of the defect. PL studies indicate that the system has C_{3v} symmetry (²E state) with possibly exhibiting dynamic Jahn-Teller effect that inhibits the EPR detection of the ²E ground state [25]. The C_{1h} symmetry configuration and the ²E ground state of C_{3v} symmetry can be described by single Slater-determinants, so we could address this issue directly at LDA level. The lowest excitation can be obtained by promoting one electron from $a_1(2)$ level to e level resulting in $a_1(1)^2 a_1(2)^1 e^2$ configuration. The possible excited states of $a_1(1)^2 a_1(2)^1 e^2$ configuration have ²A₁, ⁴A₂ and ²E multiplets. The $M_S = \frac{3}{2}$ state of ⁴A₂ multiplet can be described by a single Slater-determinant by simply aligning all the electrons spin-up on the $a_1(2)$ and e levels, thus the spin density can be determined by usual LDA calculation. We note that no Jahn-Teller effect occurs for ⁴A₂ state, so we considered only C_{3v} symmetry for this state in the calculations. We focused our research on the ground state of C_{1h} and C_{3v} symmetries,

and the 4A_2 excited state that are relevant in the recent EPR study [21]. We note here that the nitrogen dangling bond is hybridized into $a_1(2)$ but not into the e defect states, therefore, negligible spin density is expected for the 2E ground state but considerable spin polarization may be expected for the 4A_2 excited state.

First, we investigated the ground state of NV^0 . Since Jahn-Teller effect can occur, we distorted the symmetry to C_{1h} , and allowed the atoms to relax to find the energy minimum within LDA. We found that the system conserves its C_{1h} symmetry and it does not form the C_{3v} configuration. The single occupied e -level in the gap is split by 0.3 eV resulting in an occupied a' state and an unoccupied a'' state of the spin-up electrons. The neighbor N and C atoms relaxed outward from the vacant site. The nitrogen atom remained very close to the $\langle 111 \rangle$ axis even in C_{1h} symmetry, while one of the carbon atoms is considerably closer to the vacant site than the other two. Next, we constrained the system to preserve the C_{3v} symmetry during the geometry optimization in order to calculate the total energy of 2E state. We found that it is about 0.09 eV higher in energy than the Jahn-Teller distorted one. Then, we allowed the system to relax without symmetry constraints starting from the optimum C_{3v} geometry. The atoms automatically relaxed to the C_{1h} symmetry. This result indicates that C_{3v} symmetry is a local maximum. This finding seems to contradict the PL spectrum which shows 2E ground state within C_{3v} symmetry. However, we carried out quasi-static calculations at 0 K, and we did not take the vibronic states and temperature effects into account. This result shows clearly a multi-valley potential surface for the ground state of this defect as was already hinted by Davies [25]. Our calculated Jahn-Teller energy (0.09 eV) is very close to the estimation of Davies (0.14 ± 0.07 eV) based on the luminescence measurements [25]. There are three equivalent C_{1h} configurations around the vacant site rotated by 120 degrees about the C_{3v} -axis with each possessing the global minimum. At LDA-level, we can estimate the upper limit of the energy barrier between the three global minima, that is ≈ 0.09 eV. There may exist more favorable path between these global minima than through the C_{3v} configuration, so the actual barrier energy may be even lower than that. Due to the strong C-C bonds in diamond ≤ 0.09 eV energy difference can be gained even at very low temperature because this is about the zero point energy of the phonons with the highest energy (≤ 0.083 eV). This results in a motional average of the single electron between the three equivalent C_{1h} configurations, showing an effective C_{3v} symmetry. It was speculated [21, 25] that the dynamic Jahn-Teller effect is responsible for the missing EPR signal of the 2E ground state. Our calculations support this assumption.

We also investigated the 4A_2 excited state. This state has indeed much higher energy by about 0.86 eV compared to that of the low-symmetry ground state. We note that the LDA total energy differences should not be directly compared to the measured transition energies as previously discussed in Ref. 24. In this state the $a_1(2)$ defect level is polarized, thus the nitrogen atom is polarized in contrast to 2E state. This re-

TABLE I: The calculated principal values of the hyperfine tensor (columns 2 to 4) compared to the known experimental data (columns 5 to 7) in MHz. The experimental data on ${}^{15}\text{N}$ is taken from Ref. 21. The ${}^{13}\text{C}$ hyperfine signal could not be resolved in that experiment.

Atom	A_{11}	A_{22}	A_{33}	A_{11}^{exp}	A_{22}^{exp}	A_{33}^{exp}
${}^{15}\text{N}$	-23.4	-23.4	-39.0	-23.8(3)	-23.8(3)	-35.7(3)
${}^{13}\text{C}(3\times)$	60.6	61.0	126.2			

sults in considerable rearrangement of the atoms around the vacancy, namely, the nitrogen moves closer to the vacant site. We calculated the hyperfine tensors of atoms for the optimum geometry and compared to a recently found EPR center as explained in the introduction [21] (see Table I). The agreement between the calculated and measured hyperfine signal is excellent. In addition, the calculated binding energy of the NV^0 complex (≈ 3.0 eV) shows a high thermal stability, and its ($-/0$) occupation level is at about 2.0 eV above valence band edge, in line with the experimental observations [18]. Thus, we identify the EPR signal of NV^0 . We provide the hyperfine data of the three nearest carbon atom near the vacant site that has the largest hyperfine interaction. These carbon atoms may be measured by future EPR experiments when the signal to noise ratio can be reduced there.

After identification of NV^0 defect we discuss its possible role in spin physics. NV^- was successfully used to realize qubits [9, 10]. Second order correlation and EPR measurements were employed to detect individual NV^- . The resulting spin-echo signals show a rapidly oscillating function enveloped by a more slowly oscillating function [9]. The authors of Ref. 9 proposed a theory to explain this signal, and they concluded that the fast modulation frequency is due to the effective magnetization density of the electron spin felt by the ${}^{13}\text{C}$ nucleus, which is the same as the hyperfine interaction. If too many ${}^{13}\text{C}$ nuclei are involved in the process that will lead to fast decoherence of the spin-echo signal [9], therefore, the knowledge of the spin density distribution is crucial. The situation is complex for the ground state as was discussed above. At the measurement temperature an effective C_{3v} symmetry may be detected as the motional average of the three equivalent C_{1h} configurations. It is difficult to handle this situation by quasi-static simulation. We simulate this average simply by taking the optimum 2E ground state within C_{3v} symmetry. We found that the overall picture is very similar to what was found for NV^- [24]. In the ground state the spin density is mainly localized on the three nearest neighbor carbon atom of the vacant site, and the spin density decays fast as a function of the distance from the vacant site. From this point of view, a potential qubit of NV^0 would be weakly coupled to its environment and, therefore, it might present the right coherence properties like NV^- .

However, the localized spin density is not the only requirement to produce qubits. One needs to generate a superposition state and read-out the qubit states. In the case of NV^- the $M_S = 0$ of the triplet *ground state* can be optically pumped

which has much smaller hyperfine interaction with the proximal ^{13}C nucleus than the $M_S = 1$ state [9]. This effect was responsible for the collapse and revival of the electron spin coherent state. The M_S states could be read-out also optically after the measurements by using the fact that they have different fluorescence rates [9].

In NV^0 defect the optical pump can change the $S = \frac{1}{2}$ state to $S = \frac{3}{2}$ excited state, and by switching off the light excitation this can be transformed back to the $S = \frac{1}{2}$ state. The nature of the spin-flip process will be discussed shortly. The group theory analysis tells us that no spin-orbit coupling arises for the 4A_2 excited state. However, the spin-spin interaction is active, which can be given by the following effective spin-Hamiltonian for this particular system: $\hat{H}_{SS} = D'(S_z^2 - 5/4)$, where D' is the zero-field constant and S_z has the M_S eigenvalue. So, the $4 \times$ degenerate 4A_2 state will split to two double degenerate states due to spin-spin interaction resulting in the lower lying $M_S = 1/2; -1/2$ and the upper lying $M_S = 3/2; -3/2$ levels (see Fig. 1). These levels are separated by $2 \times D' = D$. $D \approx 1685$ MHz was experimentally measured by EPR [21]. According to Davies PL analysis [25] ~ 2.2 eV excitation occurs between 2E ground state to the 2A_1 excited state. We propose that the $M_S = 1/2; -1/2$ electron states of the 2A_1 excited state can relax to the $M_S = 1/2; -1/2$ sublevels of 4A_2 state with a finite probability instead of relaxing back to the ground state. While the spin-orbit interaction is not active for 2A_1 state itself the *axial spin-orbit interaction couples the 2A_1 states selectively with the $M_S = 1/2; -1/2$ 4A_2 states*. That is the source of the spin-flip process which may be further mediated by phonons in order to satisfy the energy conservation of this transition. Indeed, the threshold excitation energy of the EPR signal, 2.2(1) eV [21], is larger than the ZPL energy of 2.156 eV, and it has the highest intensity using excitation energy of about 2.5 eV. The probability of the relaxation process between the original 2E and 1A_1 ($S = \frac{1}{2}$) states should be higher than for the original 4A_2 ($S = \frac{3}{2}$) state. One may estimate from the known data of the NV^- center [26] that the duration of the direct transition process is about 10 ns, while for the spin flip process it could be about 30 ns. Therefore, the duration of the optical pumping can be relatively long in order to arrive at $M_S = 1/2; -1/2$ sublevels of 4A_2 state from the 2E ground state. The typical EPR condition for 4A_2 state is shown in Fig. 1. The small external constant magnetic field (\mathbf{B}) will split the $M_S = 1/2; -1/2$ sublevels lowering the energy of $M_S = -1/2$ state. Finally, we predict that during the optical pumping the $M_S = 1/2; -1/2$ sublevels of 4A_2 state will be *selectively* populated with somewhat higher probability for $M_S = -1/2$ because it is lower in energy. Then, the varying microwave magnetic field induce the transitions $M_S = \pm 1/2 \leftrightarrow \pm 3/2$ in the EPR measurements. This scenario can explain all the photo-EPR findings in Ref. 21.

The question arises what kind of entity can be used as a qubit from NV^0 defect. The first choice it to use simply the S -state. By optical pumping the S -state of NV^0 defect can be transformed from $1/2$ to $3/2$, and by switching off the light it can be transformed back from $3/2$ to $1/2$ with $t \ll 1$ s [21].

However, it is not probable that coherent state can be achieved for the ground state as we showed that it exhibits a dynamic Jahn-Teller effect causing a *rapidly varying effective magnetic field* for the ^{13}C nuclei around the NV^0 defect. Furthermore, the time-averaged effective hyperfine interaction of both states are very similar. This is also disadvantageous.

Another possibility is to use the M_S sublevels of the 4A_2 state as qubit. As explained above by optical pumping one can select the $M_S = 1/2; -1/2$ sublevels of 4A_2 state of the NV^0 defect with *almost equal* probability. That is not applicable for qubits. However, one can selectively set either $M_S = +3/2$ (with energy of $h\nu_1$) or $M_S = -3/2$ ($h\nu_2$) states by applying a π pulse [9] to induce the EPR transition ($\Delta M_S = \pm 1$) (see Fig. 1). *The $M_S = \pm 3/2$ states may be used as qubit*. It is clear in the above mentioned scenario that ν_1 can *only* be associated with $M_S = +3/2$ while ν_2 *only* with $M_S = -3/2$. We would like to emphasize that these metastable $M_S = \pm 3/2$ states are extremely long living (> 1 μs) because i) the 4A_2 state is the only $S = 3/2$ state, so there is no way for radiative recombination for this state ii) the $M_S = \pm 3/2$ states are *not coupled to the 2A_1 excited state at all that hinders the recombination of these states to the 2E ground state via 2A_1 excited state*. This is unique compared to the NV^- center [26] and suggests a longer lifetime of these metastable states than for the measured lifetime of the singlet metastable state in NV^- center (300 ns) [26]. We note that the $M_S = \pm 3/2$ states are very weakly coupled to the 2E ground state by *non-axial* spin-orbit interaction. However, the *non-axial* spin-orbit interaction is very small (as assumed for NV^- center [26]) and *it is too far in energy in order to mediate this process by phonons*. So, the probability of this decay is very small ensuring the very long lifetime of these states. The coherent state between these $M_S = \pm 3/2$ states and the proximate ^{13}C nuclei can certainly be maintained similar to NV^- [9]. The readout process could be very simple: by applying a π pulse again the $M_S = \pm 3/2$ states scatter to 4A_2 $M_S = \pm 1/2$ states that through the spin-orbit coupling can go back to the 2A_1 excited state, finally by radiative recombination to the 2E ground state. Therefore, the spin qubit state can be readout optically. This process can be tuned by applying the appropriate constant magnetic field to split the levels and the microwave magnetic field (π pulse) to induce transitions between the levels.

In this work we investigated the *neutral* nitrogen-vacancy defect in diamond in detail by *ab initio* LDA supercell calculations. We showed that the defect indeed shows the dynamic Jahn-Teller effect for the ground state. We identified the recently found EPR center [21], as the 4A_2 excited state of the *neutral* nitrogen-vacancy defect. That EPR center can be used to trace the NV^0 -contained nanodiamonds magnetically. We found that NV^0 is a promising candidate for realizing qubits in diamond *without the need of nitrogen donors*.

AG acknowledges support from Hungarian OTKA No. K-67886. The fruitful discussion with Jeronimo Maze is appreciated.

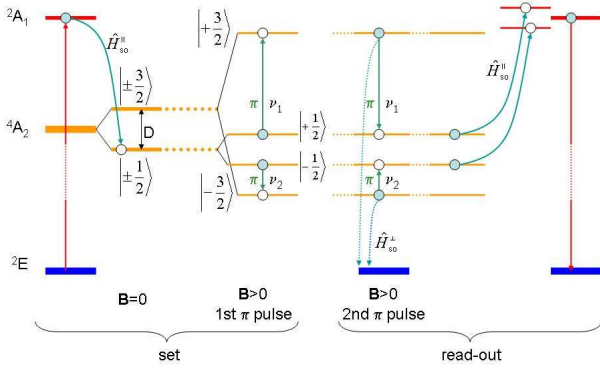


FIG. 1: (Color online) The process of the manipulation of a qubit in NV^0 defect. Straight red arrow: radiative recombination. Curved green arrow: spin-orbit coupling (\hat{H}_{SO}) possibly mediated by phonons. Grey dotted arrows represent very weak interaction. Blue straight line: microwave alternating magnetic field pulse. Filled(empty) circle: initial(final) state of the electron. Setting the qubit state: i) excitation from the 2E ground state to the 2A_1 excited state ii) spin-flip to the appropriate 4A_2 states iii) setting either $M_S = 3/2$ or $M_S = -3/2$ state by π pulse. Readout the qubit state: i) π pulse to go back to $M_S = \pm 1/2$ states ii) spin-flip to the 1A_1 state iii) radiative recombination to the 2E ground state. We show the fine structure of 4A_2 states in the absence of external magnetic field ($B=0$) (2nd column) and at $B > 0$ with typical EPR conditions in the next columns. $D \approx 1685$ MHz fine structure constant was determined by EPR [21]. The figure does not show the true scale for the sake of clarity.

[1] L. du Preez, PhD. dissertation, University of Witwatersrand, 1965.
[2] G. Davies and M. F. Hamer, Proc. R. Soc. London Ser. A **348**, 285 (1976).
[3] J. Wrachtrup, S. Y. Kilin, and A. P. Nizotsev, Opt. Spectrosc. **91**, 429 (2001).
[4] F. Jelezko, I. Popa, A. Gruber, C. Tietz, J. Wrachtrup, A. Nizotsev, and S. Kilin, Appl. Phys. Lett. **81**, 2160 (2002).
[5] F. Jelezko, T. Gaebel, I. Popa, A. Gruber, and J. Wrachtrup, Phys. Rev. Lett. **92**, 076401 (2004).

[6] F. Jelezko, T. Gaebel, I. Popa, M. Domhan, A. Gruber, and J. Wrachtrup, Phys. Rev. Lett. **93**, 130501 (2004).
[7] R. J. Epstein, F. Mendoza, Y. K. Kato, and D. D. Awschalom, Nat. Phys. **1**, 94 (2005).
[8] R. Hanson, F. M. Mendoza, R. J. Epstein, and D. D. Awschalom, Phys. Rev. Lett. **97**, 087601 (2006).
[9] L. Childress, M. V. Gurudev Dutt, J. M. Taylor, A. S. Zibrov, F. Jelezko, J. Wrachtrup, P. R. Hemmer, and M. D. Lukin, Science **314**, 281 (2006).
[10] M. V. Gurudev Dutt, L. Childress, L. Jiang, E. Togan, J. Maze, F. Jelezko, A. S. Zibrov, P. R. Hemmer, and M. D. Lukin, Science **316**, 312 (2007).
[11] R. Hanson, V. V. Dobrovitski, A. E. Feiguin, O. Gywat, and D. D. Awschalom, Science **320**, 352 (2008).
[12] J. H. N. Loubser and J. P. van Wyk, in *Diamond Research (London)* (Industrial Diamond information Bureau, London, 1977), pp. 11–15.
[13] R. Hanson, O. Gywat, and D. D. Awschalom, Phys. Rev. B **74**, 161203(R) (2006).
[14] S. Takahashi, R. Hanson, J. van Tol, M. S. Sherwin, and D. D. Awschalom, Physical Review Letters **101**, 047601 (2008).
[15] S.-J. Yu, M.-W. Kang, H.-C. Chang, K.-M. Chen, and Y.-C. Yu, J. Am. Chem. Soc. **127**, 17604 (2005).
[16] Y.-R. Chang, H.-Y. Lee, K. Chen, C.-C. Chang, D.-S. Tsai, C.-C. Fu, T.-S. Lim, Y.-K. Tzeng, C.-Y. Fang, C.-C. Han, H.-C. Chang, and W. Fann, Nature Nanotechnology **3**, 284 (2008).
[17] J. Rabeau, A. Stacey, A. Rabeau, S. Prawer, F. Jelezko, I. Mirza, and J. Wrachtrup, Nano Letters **7**, 3433 (2007).
[18] Y. Mita, Phys. Rev. B **53**, 11360 (1996).
[19] G. Davies, S. C. Lawson, A. T. Collins, A. Mainwood, and S. J. Sharp, Phys. Rev. B **46**, 13157 (1992).
[20] T. A. Kennedy, J. S. Colton, J. E. Butler, R. C. Linares, and P. J. Doering, Applied Physics Letters **83**, 4190 (2003).
[21] S. Felton, A. M. Edmonds, M. E. Newton, P. M. Martineau, D. Fisher, and D. J. Twitchen, Physical Review B **77**, 081201(R) (2008).
[22] G. Kresse and J. Furthmüller, Phys. Rev. B **54**, 11169 (1996).
[23] P. E. Blöchl, C. J. Först, and J. Schimpl, Bull. Mater. Sci. **26**, s33 (2001).
[24] A. Gali, M. Fyta, and E. Kaxiras, Physical Review B **77**, 155206 (2008).
[25] G. Davies, J. Phys. C **12**, 2551 (1979).
[26] N. B. Manson, J. P. Harrison, and M. J. Sellars, Physical Review B **74**, 104303 (2006).